Heliyon 10 (2024) e27084

Contents lists available at ScienceDirect

Heliyon

journal homepage: www.cell.com/heliyon

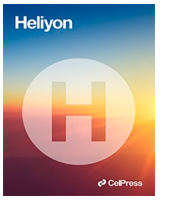

Research article

Pitavastatin induces autophagy-dependent ferroptosis in MDA-MB-231 cells via the mevalonate pathway

Wen-Juan Tang [a,1], Di Xu [b,1], Ming-Xing Liang [b], Guan-Qun Wo [c], Wen-Quan Chen [b], Jin-Hai Tang [b,**], Wei Zhang [b,*]

[a] Department of Oncology, The Affiliated Taizhou People's Hospital of Nanjing Medical University, Taizhou, 225316, PR China
[b] Department of General Surgery, The First Affiliated Hospital of Nanjing Medical University, Nanjing, 210029, PR China
[c] The First Clinical Medical College, Nanjing University of Chinese Medicine, Nanjing, 210023, PR China

ARTICLE INFO

Keywords:
Triple-negative breast cancer
Statin
Ferroptosis
Mevalonate pathway
Anticancer

ABSTRACT

Triple-negative breast cancer (TNBC) is more prone to recurrence and metastasis relative to other subtypes of breast cancer, leading to an extremely poor prognosis. The increasing potential chemoresistance of TNBC patients is mainly due to that tumor cells escape from apoptosis. In recent years, statins have demonstrated extensive anti-tumor effects. It is worth noting that statins have more effective anti-tumor effects on TNBC cells and drug-resistant breast cancer cells. Therefore, this study examines the superior cytotoxic effects of statins on TNBC cell lines and further explores their potential therapeutic mechanisms. We detected different cell phenotypes and found that statins significantly reduced the cell viability of TNBC cells. Specifically, pitavastatin showed an obvious induction in cell death, cell cycle arrest and oxidative stress in TNBC MDA-MB-231 cells. The reversal effect of iron chelator desferrioxamine (DFO) on the morphological and molecular biological changes induced by pitavastatin has revealed a new mode of cell death induced by pitavastatin: ferroptosis. This ferroptotic effect was strengthened by the decreased expression of glutathione peroxidase 4 (GPx4) as well as newly discovered ferroptosis suppressor protein 1 (FSP1). The data showed that ferroptotic death of MDA-MB-231 cells is autophagy-dependent and mediated by the mevalonate pathway. Finally, we found that therapeutic oral doses of statins can inhibit the growth of transplanted tumors, which establishes statins as a potential treatment for TNBC patients. In conclusion, we found pitavastatin could induce autophagy-dependent ferroptosis in TNBC cells via the mevalonate pathway which may become a potential adjuvant treatment option for TNBC patients.

1. Introduction

Breast cancer has now overtaken lung cancer as the most commonly diagnosed cancer. Among all breast cancer cases, triple-negative breast cancer (TNBC) composes about 10–20% and is more common in premenopausal patients, but is being diagnosed in younger and younger patients [1]. Patients with TNBC are more prone to local recurrence [2] and distant metastasis [3] when

* Corresponding author.
** Corresponding author.
E-mail addresses: jhtang@njmu.edu.cn (J.-H. Tang), weizhang@njmu.edu.cn (W. Zhang).
[1] These authors have contributed equally to this work.

https://doi.org/10.1016/j.heliyon.2024.e27084
Received 26 October 2023; Received in revised form 4 February 2024; Accepted 23 February 2024
Available online 24 February 2024

compared with other subtypes due to their higher invasiveness and the lack of targeted therapy, leading to a poor prognosis of TNBC patients. Commonly used chemotherapeutics for TNBC patients usually initiate apoptosis. Unfortunately, TNBC frequently tends to evade apoptosis and develop chemotherapy resistance, especially as it progresses [4]. The severe situation revealed by the epidemiology of TNBC requires a deeper exploration of its treatment strategies [5].

Discovering other alternative modes of cell death provides more opportunities for the efficient treatment of TNBC patients. Ferroptosis, a relatively new cell death mode, is distinctly different from other forms of regulatory cell death in morphological and molecular biology indicators [6]. The morphological changes of ferroptosis are mainly manifested in the cell membrane and mitochondria, where mitochondria become smaller, cristae decrease or disappear, and the outer membrane subsequently ruptures. The accumulation of lipid peroxides destroys the redox balance in the cell and triggers cell death, which is the essential biological feature of ferroptosis. Glutathione peroxidase 4 (GPx4), a membrane lipid repair enzyme, plays an important role by transferring the peroxide group (-OOH) of polyunsaturated fatty acid (PUFA) to the glutathione (GSH). If GPx4 fails, ferroptosis ensues because of the accumulation of reactive oxygen species (ROS) [7]. Recently, researchers found that ferroptosis suppressor protein 1 (FSP1) also participates in the inhibition of ferroptosis in parallel with GPx4 [8,9]. Studies have shown that drug-resistant cancer cells rely on GPx4 activity to eliminate lipid peroxides and thereby selectively sensitive to the ferroptosis due to their exhibition of high mesenchymal states [10,11]. Interestingly, a study found that when compared with ER-positive breast cancer, TNBC is more sensitive to ferroptosis due to the expression of ACSL4 (acyl-CoA synthetase long chain family member 4), which is a key enzyme that regulates lipid composition and maintains membrane architecture [12]. Therefore, triggering ferroptosis could be an effective treatment strategy for TNBC patients.

Statins are inhibitors of HMG-CoA reductase (HMGCR), a rate-limiting enzyme in cholesterol synthesis. Several studies have found that statins play positive roles in a variety of tumors [13]. The anti-tumor efficiency of statins may depend on statin type and the target tumor type [14]. In breast cancer, statins have been reported to show synergistic anti-tumor effects with radiotherapy [15], chemotherapy [16] and endocrine therapy [17]. More importantly, a meta-analysis shows that lipophilic statins are beneficial for the clinical outcomes of breast cancer patients [18]. Mechanisms such as inhibition of proliferation and cell cycle, and induction of apoptosis have been discussed in regards to statins [19,20]. Interestingly, statins have better specific anti-tumor effects in drug-resistant cells and TNBC cells, which demonstrate dependence on GPx4 and thereby confers increased sensitivity to ferroptosis [10,11]. Therefore, we hypothesized that ferroptosis has a certain significance in the anti-tumor effect of statins. To reveal the mechanism(s) of statins, we detected the significance of iron on the anti-tumor effect of pitavastatin on the TNBC cell lines. The results indicated that co-treatment with the iron chelator, desferrioxamine (DFO) reversed the cell cycle arrest, cell death, and elevated ROS induced by pitavastatin, reflecting that it is iron-dependent. Overall, these findings demonstrate the occurrence of ferroptosis in human TNBC MDA-MB-231 cells.

Preclinical animal experiments are the cornerstone of basic research and translational research. However, the dosages and methods of statin administration in existing studies are not uniform, resulting in poor clinical predictability. We conducted experiments based on human administration methods and appropriate dosages for the first time and revealed the effectiveness of safe therapeutic dosage levels of statins on tumor-bearing mice *in vivo*. This study establishes statins as a promising anti-cancer therapy for refractory TNBC patients.

2. Materials and methods

2.1. Cell culture and reagents

Human TNBC cell lines (MDA-MB-231, HCC1806, BT-549, Hs578T, and SUM1315) were purchased from the Shanghai Academy of Biological Sciences, Chinese Academy of Sciences (Shanghai, China). MDA-MB-231 and HCC1806 were cultured in L-15 medium (BasalMedia, Shanghai, China) and RPMI-1640 medium (KeyGEN BioTECH, Nanjing, China) supplemented with 10% fetal bovine serum (FBS) (Gibco, New York, USA) separately. Hs578T, and SUM1315 were both cultured in DMEM medium (KeyGEN BioTECH, Nanjing, China) supplemented with 10% FBS. BT-549 was cultured in DMEM medium supplemented with 20% FBS. All cell lines were incubated at 37 °C in 5% CO_2, except for MDA-MB-231 which was grown in ambient air. Four statins were purchased from Aladdin (Shanghai, China). Dimethylsulfoxide (DMSO) was purchased from Solarbio (Beijing, China). The maximum volume ratio of DMSO was used as a mock control. DFO and mevalonate (Meva) were purchased from Sigma-Aldrich (St. Louis, MO, USA). Anti-FSP1, anti-p53 and anti-GAPDH were purchased from ProteinTech (Chicago, USA). Anti-GPx4, Anti-LC3B, and Anti-HMGCR were purchased from Abcam (Cambridge, UK), Cell Signaling Technology (CST) (Danvers, MA, USA), and Santa Cruz (CA, USA) separately. Goat anti-Rabbit IgG-HRP and Goat anti-Mouse IgG-HRP were purchased from Beyotime (Shanghai, China).

2.2. Cell administration

Reagents were configured with DMSO as high concentration solutions for storage, typically 10 mM. Cell suspension was seeded in the plate at an appropriate density and incubated in the corresponding medium overnight. The next day, calculated volume of the reagent was added into the supernatant, then the whole plate was incubated at 37C for a certain period after slowly and thoroughly mixed. The maximum volume ratio of DMSO was used as a mock control.

2.3. Cell counting Kit-8 (CCK-8) assay

100 μL of human TNBC cell suspension was seeded in a 96-well plate at an appropriate density per well and incubated in the corresponding complete medium overnight. The next day, 100 μL of 2 × concentration gradient of statins (1, 2, 4, 8, 16, 32, 64, 128 μM) were added into each column. 48 h later, 10 μL of CCK-8 (APExBio, Houston, USA) solution was dropped to experimental wells and then the whole plate was incubated at 37 °C for 1–4 h. The optical density (OD) value was then measured through a microplate reader (Molecular Devices, USA) at 450 nm and represented a readout of cell viability.

2.4. Cell cycle analysis

TNBC cell lines were seeded in a 6-well plate at an appropriate density per well and incubated in the corresponding complete medium overnight. The next day, cells were treated with 5 μM pitavastatin for 36, 48, and 60 h. Cells needed to be fixed with absolute ethanol at −20 °C for at least 24 h upon harvesting. On the day of testing, we centrifuged the fixed cells to discard the ethanol and added 3 mL of phosphate buffered saline (PBS) to hydrate the cells. Then, cells were centrifuged again to discard the supernatant, suspended in 500 μL of DNA staining solution with propidium iodide (PI), and then incubated for 30 min in the dark. In the end, the prepared stained cells were collected by a Flow cytometer (Beckman Coulter, USA) for assessment.

2.5. Cell apoptosis analysis

Cell apoptosis analysis was detected via Annexin V-FITC and PI staining Kit (Beyotime, Shanghai, China). After treated with 5 μM pitavastatin for 36, 48, and 60 h, the TNBC cell lines were collected, suspended in 500 μL of binding buffer and stained with the probes mentioned above. Finally, cell apoptosis analysis was analyzed through the Flow cytometer described above. As the cell debris clusters were also important for us, we classified all except double-negatives as dead cells. The formula to calculate the cell death is as follows: percentage of cell debris clusters (First Quadrant) + percentage of late apoptotic cells (Second Quadrant) + percentage of early apoptotic cells (Fourth Quadrant).

2.6. ROS level detection

Intracellular ROS level was measured via dichlorofluorescein diacetate (DCFH-DA) (Sigma-Aldrich, St. Louis, MO, USA) probe. After treated with 5 μM pitavastatin for 12, 24, and 48 h, the whole plate of MDA-MB-231 cells were treated with 5 μM DCFH-DA (1:1000 dilution) for 30 min. Prepared cells were then harvested and finally suspended in incomplete L-15 medium to be detected via flow cytometry (Beckman Coulter, USA). We aggregated the acquired data onto a specific image for analysis.

2.7. Transmission electron microscopy (TEM) imaging

Briefly, the cells were trypsinized and then fixed in 5% glutaraldehyde solution at 4 °C overnight. Then, all subjects were gradually dehydrated in ethanol. After embedding, samples were sectioned and double-stained with 3% uranyl acetate-lead citrate for observation on the TEM (JEM-1010, JEOL, Japan).

2.8. Western blot (WB)

Cellular soluble protein was prepared by lysis buffer (Solarbio, Beijing, China) containing Phenylmethylsulfonyl Fluoride (PMSF) (Beyotime, Shanghai, China) (100:1) on ice. Then, the lysate and loading buffer were mixed and boiled to prepare protein samples. Protein concentration of the samples was detected via Bradford Protein Assay Kit (Beyotime, Shanghai, China). Briefly, group of samples were separated on SDS-polyacrylamide gels using electrophoresis and then electro-transferred to the PVDF membranes (Millipore, USA). After blocked with Quick Block (Beyotime, Shanghai, China), the membranes were incubated at 4 °C overnight with primary antibodies (1:400 anti-FSP1, 1:1000 anti-GPx4 and anti-LC3B, 1:2000 anti-p53, 1:10000 anti-GAPDH). After washed with Tris-buffered saline containing 0.05% (v/v) Tween-20 (TBST) three times, those PVDF membranes were incubated with secondary antibodies (1:1000 Goat anti-Rabbit IgG-HRP and Goat anti-Mouse IgG-HRP) for 1 h at room temperature the next day. Lastly, Enhanced Chemiluminescent (ECL) Kit (Beyotime, Shanghai, China) was used to detect signals under ChemiDoc™ Touch Imaging System (Bio-Rad, USA). The chemiluminescence was read out and represented the expression of the target.

2.9. In vivo experiments animal experiments

40 female BALB/c nude mice, 6 week old, were obtained from Charles River (Beijing, China). The MDA-MB-231 cell suspension, mixed with Matrigel (BD, Franklin Lakes, NJ, USA) in advance, was injected. into the breast pads at a final quantity of 5.0×10^6 cells per mouse to establish orthotopic xenografts models. Upon the tumor grew to the macroscopic size of approximately 30 mm^3, the subjects were divided into four groups randomly: Saline, Fluvastatin (8.22 mg/kg/d), Pitavastatin (0.411 mg/kg/d), and Simvastatin (4.11 mg/kg/d). Then, tumor-bearing mice (8 per group) took statins orally by daily gavage for 20 days. Tumor volume which is calculated by $a \times b^2/2$, where a and b are the largest and smallest diameters of the tumor, respectively. Bodyweight of the mice were measured every three days. The end of the animal experiments was when the mice were sacrificed and the tumors were taken out and

photographed. Hematoxylin-eosin (H&E) staining of the main organs was further performed to evaluate the safety of statins.

2.10. Hematoxylin-eosin (H&E) staining

When the mice were sacrificed, we removed main organs and fixed them in 10% formalin. Then, all tissues were gradually dehydrated in ethanol and embedded in paraffin wax blocks. Paraffin blocks were then cut into 4 μm thick sections. After dewaxed in xylene, gradually dehydrated in ethanol and washed, the prepared sections were stained and observed by optical microscope (Zeiss, Germany).

2.11. Immunohistochemical staining (IHC)

Tissue slides were heated in 60 °C for 2 h. Next, they were deparaffinized in xylene twice for 15 min respectively. And then, graded ethanol from 100% to 70% was used to rehydrated. After washed in PBS for 3 min triple times, tissue sections were put in 10 mM citric acid buffer (pH = 6.5), heating up to boiling lasting for 10 min in order to unmask antigens completely. 3% hydrogen peroxide was applied to quench endogenous peroxidase for 10 min after tissue section cooling to room temperature. After washed in PBS for 3 min triple times, the slides were blocked in 10% goat serum for 30 min at room temperature to remove nonspecific binding and then incubated with primary antibodies against Ki-67 (1:1000, ab15580, Abcam), FSP1 (1:500, 20886-1-AP, Proteintech), GPX4 (1:250, ab125066, Abcam) and HMGCR (1:500, 13533-1-AP, Proteintech) at 4 °C overnight. The next day, after washed triple times, the tissue sections were incubated with secondary antibodies (Biotin-labeled sheep anti-mouse or rabbit IgG) for 10 min. After washed triple times, streptomyces anti-biotin peroxidase was added to incubate for 10 min. Then DAB detection Kit (DAB-2031, MXB) was used to detect target protein in tissue section. And tissue sample was counterstained with hematoxylin to emerge cell nucleus. Expression was scored according to signal intensity and distribution. Evaluation of immunostaining was performed independently by two experienced pathologists.

2.12. Quantification of the mevalonate pathway metabolites

Liquid chromatography mass spectrometry (LC-MS/MS-004 6500+LC-MS 6500+, AB SCIEX, USA) was applied to analyze all metabolites. Standard chemicals isopentenyl pyrophosphate (IPP) and squalene were purchased from Sigma-Aldrich (USA) and Macklin Biochemical Co., Ltd. (Shanghai, China), respectively. Coenzyme Q10 (CoQ_{10}) and cholesterol were both obtained from Yuanye Bio-Technology (Shanghai, China).

MDA-MB-231 and SUM1315 cells were dealt with or without 5 μM pitavastatin in absence or presence of 1 mM mevalonate. After 48 h, 1×10^6 cells from each group were harvested and resuspended in 200 μL of PBS. Repeated freeze-thaw cycles were undertaken for thorough cell lysis. The cell suspension was collected in EP tubes and 1000 μL of n-hexane was added and ground in a prechilled mortar and pestle. The tissue suspension was then centrifuged for 5 min at 12,000 rpm and 4 °C. 800 μL of supernatant was moved to clean EP tubes and extracted twice by 1000 μL of n-hexane before vacuum rotary drying. The cell extract was finally resuspended in 200 μL of methanol-ethanol solution (methanol: ethanol 1:4 v/v) and centrifuged at 12,000 rpm for 5 min at 4 °C. Finally, metabolomics analyses were carried out on 100 μL of the supernatant.

To prepare the tumor samples for metabolomics analyses, tumors from the mice were dissected and washed with sterile PBS. Tissue samples were accurately weighed at 25 mg and ground in 500 μL of cold pure water. The tissue suspension was then centrifuged at 12,000 rpm (4 °C) for 5 min. 100 μL of supernatant was moved to EP tubes and extracted twice by 1000 μL of n-hexane solution before vacuum rotary drying. Tissue extract was finally resuspended in 200 μL of methanol-ethanol solution (methanol: ethanol 1:4 v/v) and centrifuged for 5 min at 4 °C and 12,000 rpm. Metabolomics analyses were performed on 100 μL of the supernatant. Each detection was repeated at least three times. Each symbol represents the mean ± SD of three experiments.

For the analysis of IPP, a Triart C18 column (YMC, 150 × 4.6 mm, 3 μm) was applied. Phase A 10 mM ammonium hydrogencarbonate solution (pH = 11) and phase B methnol were used as the mobile phase at 0.6 mL/mL and gradient elution. A Poroshell 120 EC-C18 column (Agilent, 150 × 4.6 mm, 4 μm) was chosen for the measurement of CoQ_{10}. Phase A enthanol containing 0.1% formic acid and phase B methnol were set as the mobile phase at 0.6 mL/mL and gradient elution. Cholesterol and squalene were both measured using an Acquity UPLC BEH Amide column (Waters, 100 × 2.1 mm, 1.7 μm). Phase A water and phase B methnol were used as the mobile phase at 0.3 mL/mL and gradient elution. The column temperature was set at 30 °C and injection volume was 10 μL. Under multiple reaction monitoring (MRM) mode, Electrospray ionization mass spectrometry (ESI-MS) was used to analyze mevalonate pathway metabolites. The analysis of the spectra analysis was done by comparing with internal reference compounds.

2.13. Statistical analysis

Data were expressed as mean ± standard deviation (SD). The significance of our data was measured by GraphPad Prism 8.0 (GraphPad Software, CA, USA). The significance of multiple groups was calculated through One-way ANOVA. The significance of two groups was calculated through Student's T-Test. $P < 0.05$ was considered significant versus control group.

3. Results

3.1. Statins reduce cell viability of TNBC cell lines

To explore the effect of statins on the cell viability of TNBC cell lines, we first selected four statins including atorvastatin, fluvastatin, simvastatin, and pitavastatin, and five TNBC cell lines including MDA-MB-231, HCC1806, BT-549, Hs578T, and SUM1315. Four statins had a dose-dependent inhibition on the cell viability of all five TNBC cell lines as shown in Fig. 1. In comparison, they had the weakest inhibition on HUVEC, reflecting their safety and selectivity. The IC50 values were calculated using GraphPad Prism, and the data showed that pitavastatin, a new lipophilic statin, had the highest efficiency. Thus, pitavastatin was chosen for the follow-up experiments.

3.2. Pitavastatin induces cell cycle arrest and cell death in TNBC cell lines

The cell cycle plays an important role in tumor progression [21] and may be used as a therapeutic target. We thus tested the effect of pitavastatin on the cell cycle of TNBC cell lines via flow cytometry. As shown in Fig. 2, pitavastatin significantly changed the proportion of cells at the G1 and S phase, except for SUM1315. This result indicates that pitavastatin can induce G1 phase arrest in the TNBC cell lines. The previously-mentioned proliferation inhibition might demonstrate the cytotoxicity of pitavastatin, so we explored the effect of pitavastatin on cell death in TNBC cell lines using Annexin V-FITC/PI double staining. As shown in Figs. 3, 5 μM pitavastatin resulted in significant cell death in TNBC cell lines at 60 h. Specifically, the results demonstrated a much higher proportion of cell debris compared to apoptosis, as such, other mechanisms besides apoptosis need to be investigated. We further studied the anti-tumor mechanism of pitavastatin to better understand how statins reduce cell viability most in MDA-MB-231.

3.3. Pitavastatin induces iron-dependent cell death in MDA-MB-231 cells

An important mechanism of programmed cell death is oxidative stress. Once redox balance is destroyed, ROS can induce DNA damage, and cell death [22]. We firstly detected the intracellular ROS level and found that pitavastatin increased ROS levels in MDA-MB-231 cells (Fig. 4(a)). Further, to explore whether pitavastatin induced mitochondrial functional damage in MDA-MB-231 cells, we detected the mitochondrial membrane potential (MMP) through the JC-1 probe. As shown in Fig. 4(b), pitavastatin decreased the ratio of red:green fluorescence of JC-1, which means that pitavastatin reduced the MMP of MDA-MB-231 cells. Similarly, it could be observed that the red fluorescence reduced and the green fluorescence increased in MDA-MB-231 cells after pitavastatin treatment under a fluorescence microscope (Fig. 4(c)). The aforementioned results reveal that pitavastatin can induce oxidative stress through the mitochondrial pathway in MDA-MB-231 cells, which may partially contribute to its anti-cancer effect. Besides, we wanted to know

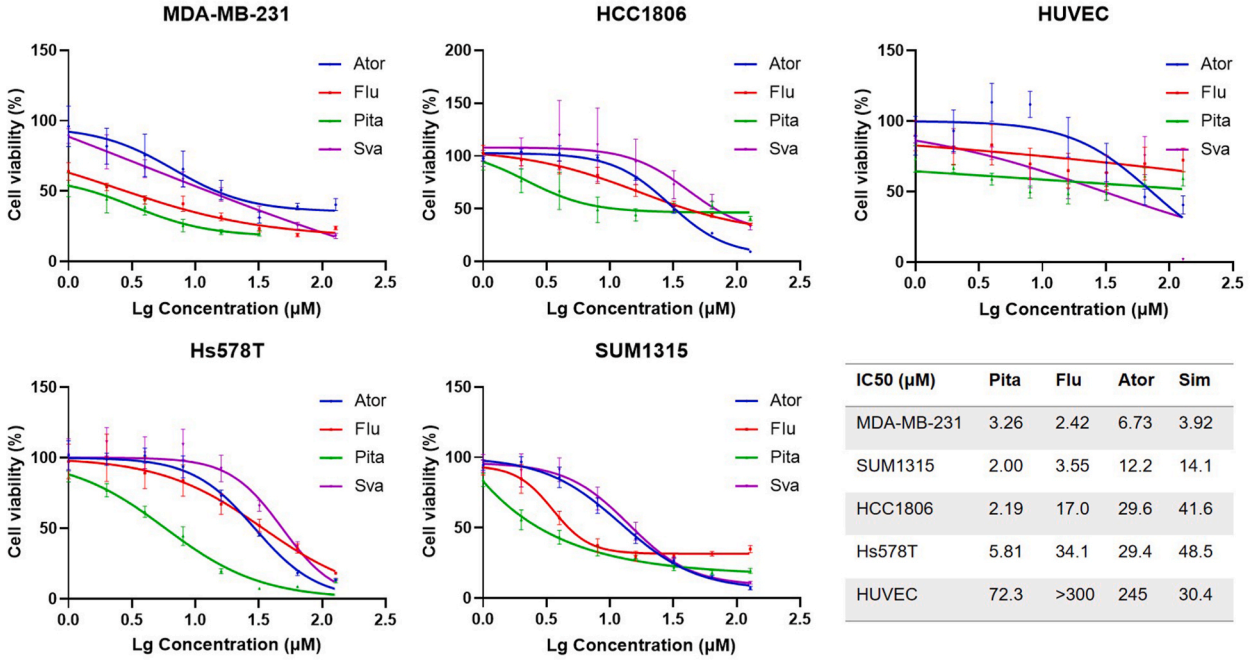

IC50 (μM)	Pita	Flu	Ator	Sim
MDA-MB-231	3.26	2.42	6.73	3.92
SUM1315	2.00	3.55	12.2	14.1
HCC1806	2.19	17.0	29.6	41.6
Hs578T	5.81	34.1	29.4	48.5
HUVEC	72.3	>300	245	30.4

Fig. 1. Effect of statins on TNBC cell viability. Human TNBC cell lines and HUVEC were treated with four statins (Atorvastatin (Ator), Fluvastatin (Flu), Simvastatin (Sim) and Pitavastatin (Pita)) for 48 h at different concentrations. The X-axis depicts statins concentration in a log10 scale. Table represented average IC50 (50% inhibiting concentration) values (unit: μM) of four statins upon 48 h treatment.

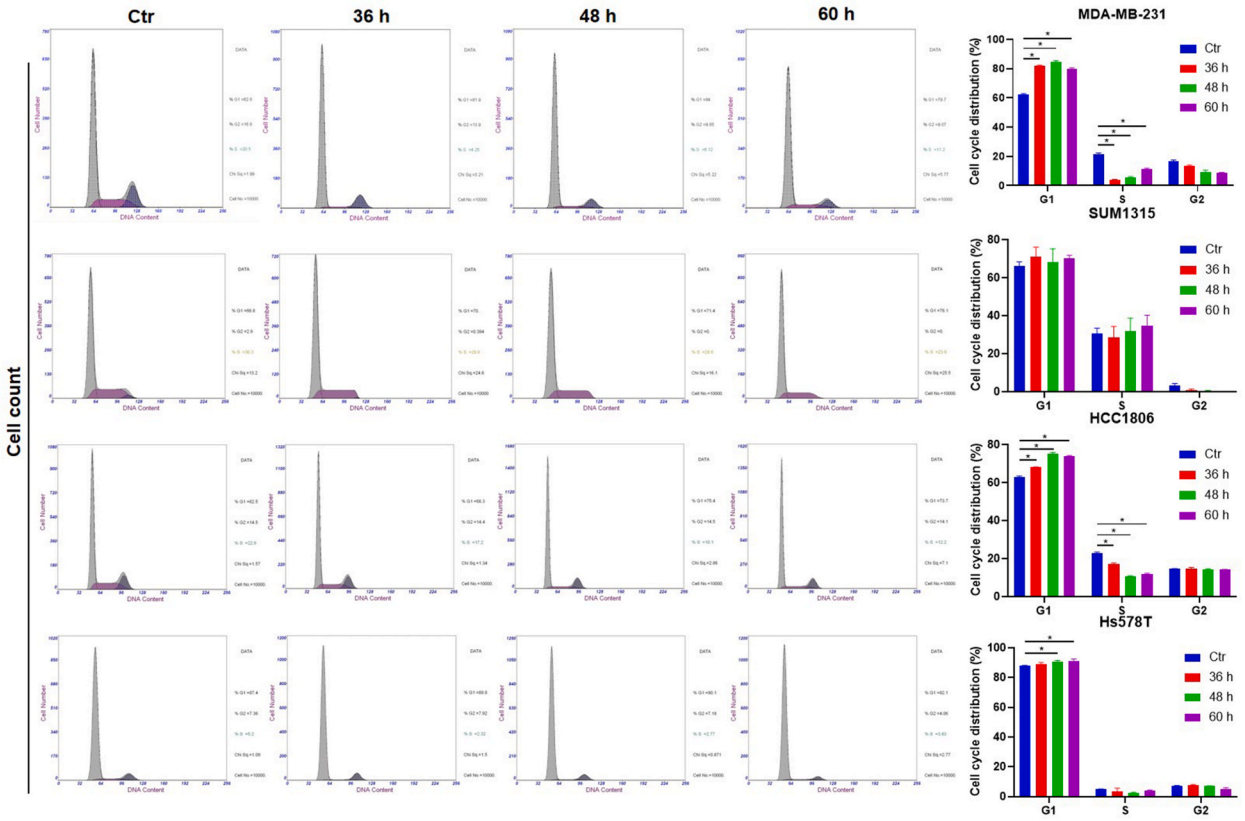

Fig. 2. Effect of pitavastatin on cell cycle positioning in TNBC cell lines. Four TNBC cell lines were plated and treated with 5 μM pitavastatin for 36 h, 48 h, and 60 h. An equal volume ratio of DMSO was always used as a mock control. Cell cycle status was assessed by PI staining. Error bars represented the mean ± SD of at least three independent experiments. $*P < 0.05$. Values of P were generated by Two-way ANOVA.

the morphological changes associated with pitavastatin treatment on MDA-MB-231 cells. We thus observed cell morphology under optical and electron microscopes. As shown in Fig. 4(d), pitavastatin could transform the adherent MDA-MB-231 cells into round, shiny, and weakly-adherent cells. Under the TEM, it could be seen that the secretory vesicles of the cell membrane are reduced and the intracellular vacuoles are increased. We also observed shrunken mitochondria and notably fewer cristae in the pitavastatin group.

Excessive oxidative stress has been implicated with the initiation of ferroptosis. The aforementioned morphological changes and biological behaviors indicate that ferroptosis may partially contribute to the cell death caused by pitavastatin. To confirm the occurrence of ferroptosis in MDA-MB-231 cells, we further explored the importance of intracellular iron (Fe^{2+}) in the action of pitavastatin. DFO, a classic inhibitor of ferroptosis was used to conduct the follow-up experiments. As shown in Fig. S1, Fig. 4(e) and Fig. S2, DFO reversed the G1 phase arrest, reduced the cell death and completely inhibited the intracellular ROS level increased by pitavastatin. The above results revealed that pitavastatin induced an iron-dependent cell death mode.

3.4. Pitavastatin induces autophagy-dependent ferroptosis in MDA-MB-231 cells

GPx4 activity, a membrane lipid repair enzyme, is an important molecular marker of ferroptosis, and its inhibition can lead to the accumulation of ROS and ferroptosis. Recently, researchers found that FSP1 also participates in the inhibition of ferroptosis in parallel with GPx4. As shown in Fig. 5(a) and (b), the expression of GPx4 and FSP1 were both significantly decreased in MDA-MB-231 cells after pitavastatin treatment and this could also be reversed by DFO. In general, pitavastatin induced ferroptosis in MDA-MB-231 cells.

Upon observing the morphological changes of pitavastatin, we could identify many autolysosomes in MDA-MB-231 cells under TEM (Fig. 5(c)). Autophagy is a process in which cytoplasmic LC3 (LC3-I) will enzymatically digest some peptides and transform into membrane type (LC3-II) [23]. We further verified the induction of autophagy through Western blotting. As shown in Fig. 5(d), the ratio of LC3-II/I was increased, reflecting the regulation in response to oxidative stress in MDA-MB-231 cells treated with pitavastatin. It is reported that excessive induction of autophagy can promote ferroptosis as a result of iron accumulation and lipid peroxidation [24]. We compared the sequence of autophagy and ferroptosis in MDA-MB-231 cells after pitavastatin treatment. It was found that autophagy occurred earlier than ferroptosis at the level of protein expression, and DFO could not reverse pitavastatin-induced autophagy, suggesting that autophagy exists independently of ferroptosis in MDA-MB-231 cells. We speculated that the ferroptosis induced by pitavastatin might also be autophagy-dependent. At least to some extent, autophagy could strengthen the ferroptosis induced by

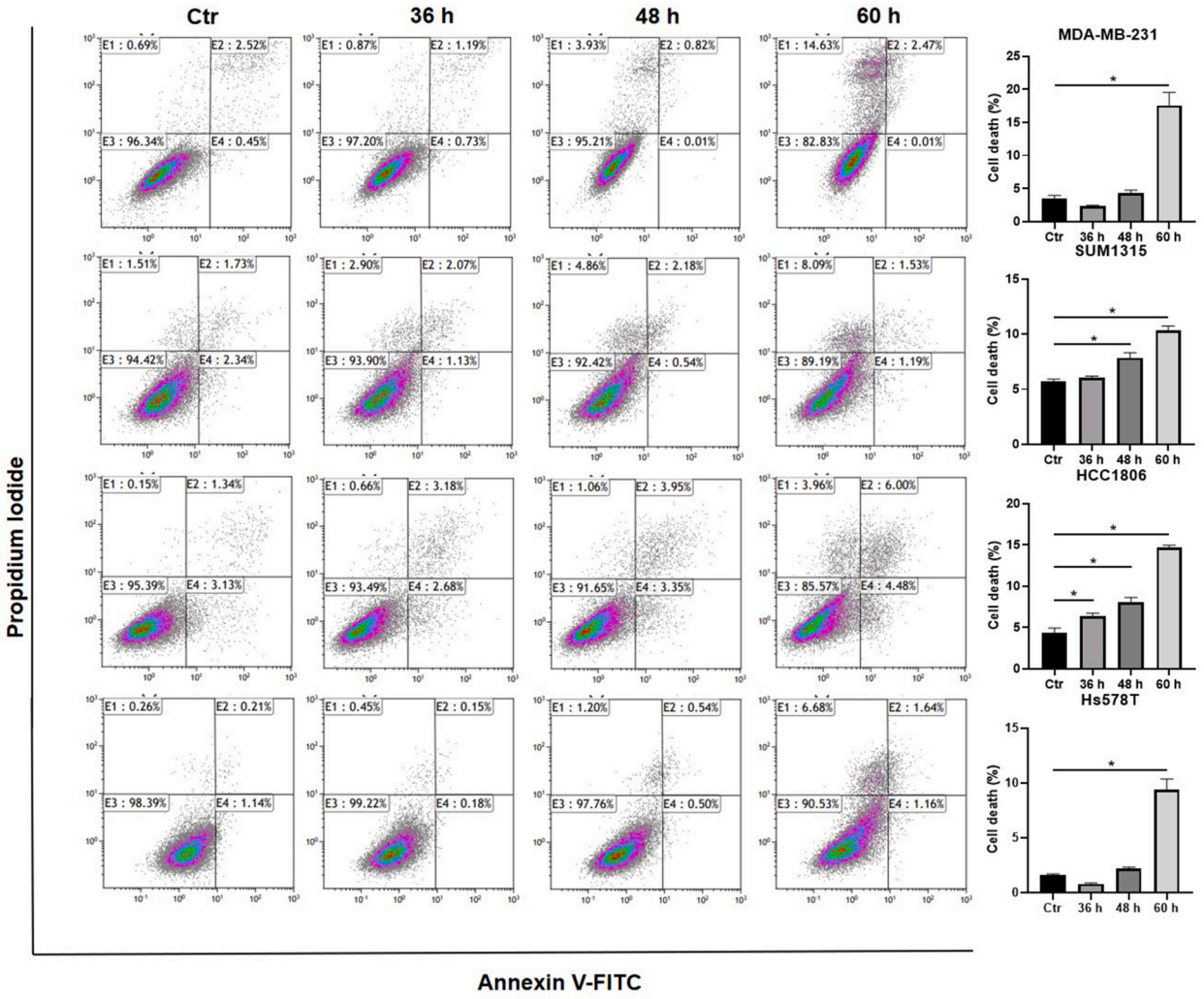

Fig. 3. Pitavastatin induces cell death in TNBC cells. TNBC cell lines were plated and treated with 5 μM pitavastatin for 36 h, 48 h, and 60 h. Analysis of cell death was performed through flow cytometry by Annexin V-FITC and PI staining. Error bars represented the mean ± SD of at least three independent experiments. $*P < 0.05$. Values of P were generated by One-way ANOVA.

pitavastatin. To address this question, we detected the effect of autophagy inhibitor chloroquine (CQ). As shown in Fig. S3, CQ significantly inhibited ferroptosis-associated lipid ROS accumulation in MDA-MB-231 cells.

3.5. Pitavastatin induces ferroptosis in MDA-MB-231 cells via the mevalonate pathway

It is widely believed that statins, a class of LDL-cholesterol lowering drugs take HMGCR, a rate-limiting enzyme of cholesterol synthesis, as the direct target. While mevalonate, an intermediate in the synthesis of cholesterol, is involved in important metabolic pathways [25]. Statins can directly reduce the synthesis of mevalonate [26] and its supplementation can partially reverse the effects of statins [19]. To further test that the cytotoxic effect of pitavastatin is due to the inhibitory of HMGCR activity, we add back mevalonic acid. As shown in Fig. 6(a) and (b), pitavastatin-induced cytotoxicity and reduction in GPx4 and FSP1 expression were prevented by mevalonate. Thus, we confirmed that pitavastatin induces ferroptosis in MDA-MB-231 via the mevalonate pathway. Furthermore, metabolomics analysis of intermediates downstream of mevalonate including IPP, squalene, cholesterol and CoQ_{10} was performed via liquid chromatography mass spectrometry (LC-MS) coupled to ESI (n = 3, mean ± SEM). The results showed pitavastatin induces inhibitory effect on mevalonate pathway intermediates in both SUM1315 and MDA-MB-231 cells (Fig. 6(c)). These responses were rescued by the supplemention of 1 mM mevalonate. As shown in Fig. 6(d), the addition of mevalonate abrogated the inhibitory effect of pitavastatin on IPP and CoQ_{10} and subsequently eliminated the inhibitory of pitavastatin on GPx4 and FSP1 activity. Moreover, it is reported that squalene accumulation in cancer cells sensitized them to ferroptosis stimulated by GPx4 inhibitors [27]. The rescue of squalene also prevented ferroptosis induced by pitavastatin.

As shown in Fig. 6(e), the Cancer Genome Atlas (TCGA) database showed that the expression of HMGCR was lower in TNBC tissues

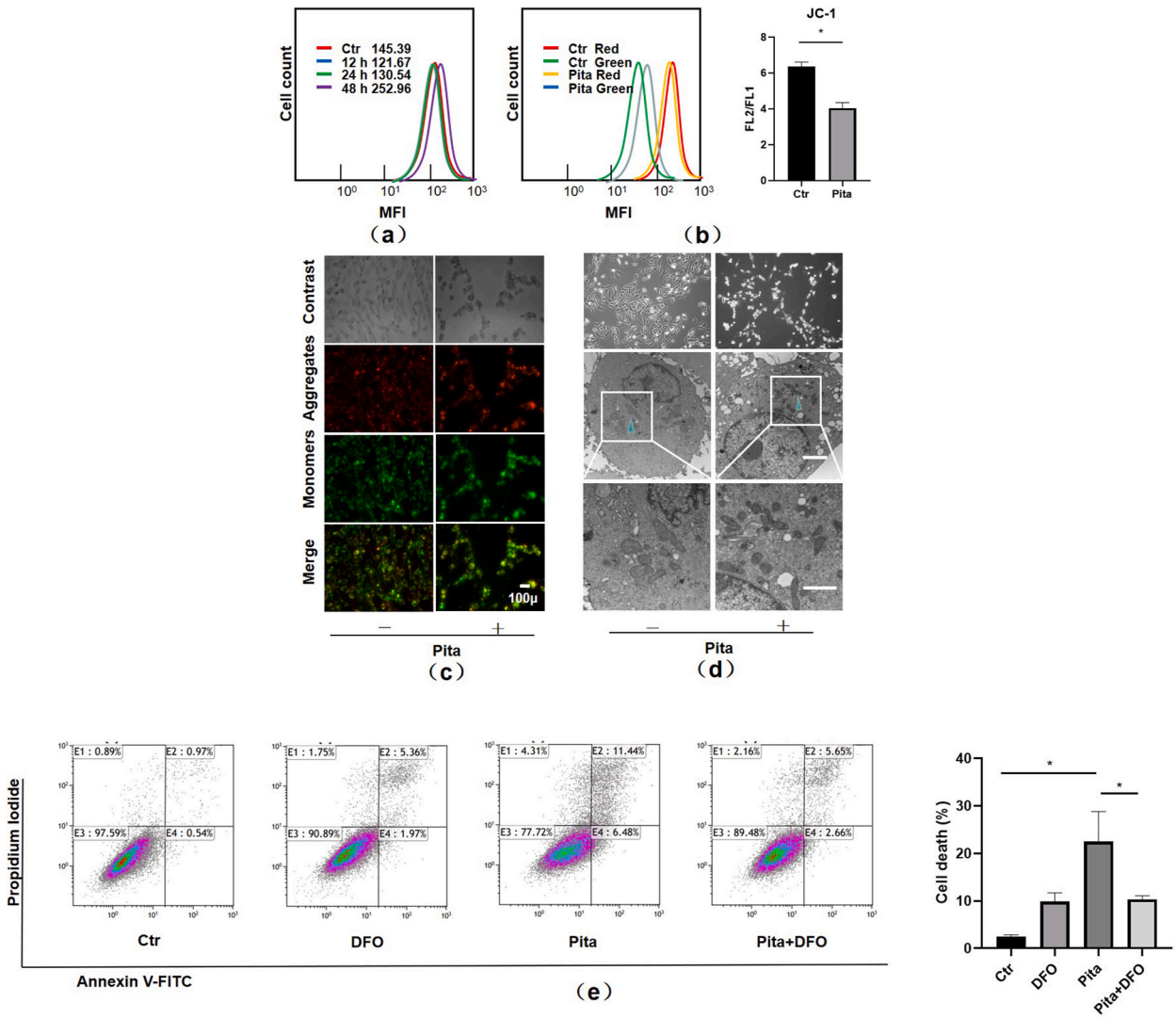

Fig. 4. Pitavastatin induces ROS production and mitochondrial damage in MDA-MB-231 cells. MDA-MB-231 cells were plated and treated with 5 μM pitavastatin for 12 h, 24 h, and 48 h. (a) Analysis of intracellular ROS level was performed by DCFH-DA staining and counted by mean fluorescence intensity (MFI) through flow cytometry. MMP was detected by JC-1 through flow cytometry (b) and fluorescence microscope (100 ×) (c) for the 48 h pitavastatin-treated cells. The blue arrow indicates the mitochondria. (d) Morphological images were taken under an optical microscope (100 ×) and TEM (10000 × , 30000 ×) for the 48 h pitavastatin-treated cells. (e) MDA-MB-231 cells were plated and treated with 5 μM pitavastatin with or without 50 μM DFO, which was added 2 h before pitavastatin treatment. Cell apoptosis was measured via Annexin V-FITC/PI double-staining at 60 h. Error bars represented the mean ± SD of at least three independent experiments. $^{*}P < 0.05$. (For interpretation of the references to colour in this figure legend, the reader is referred to the Web version of this article.)

than other breast cancer subtypes. Previous studies have found that high expression of HMGCR shows a better prognosis for the patients [28,29], which is consistent with our analysis. In 2011, Lehmann et al. found that TNBC is a group of mixed breast cancers, which can be subdivided into different types [30]. We further distinguished the gene expression level of HMGCR in those different types. It was shown that the expression of HMGCR was very low in mesenchymal stem-like (MSL) TNBC (Fig. 6(f)). This may explain why MDA-MB-231, which corresponds to the MSL type, was sensitive to statins. These results indicate the advantages of statins for the treatment of invasive breast cancer. We hope to identify breast cancer patients who will benefit from statins and discover new prognostic markers.

3.6. Statins inhibit the progression of TNBC in vivo

The dose of drugs is extremely important in *vivo* research. As FDA-approved drugs, the daily oral therapeutic doses of fluvastatin, pitavastatin, and simvastatin are 40, 2, and 20 mg for adults weighing 60 kg, respectively. We used these doses to calculate the daily

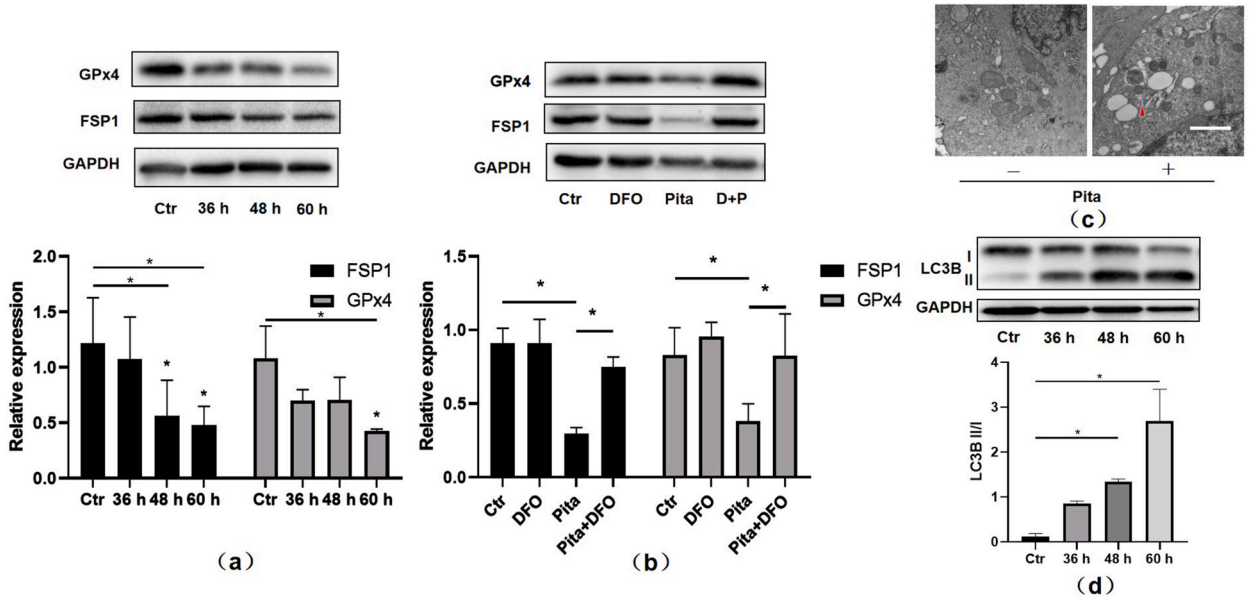

Fig. 5. Pitavastatin induces autophagy-dependent ferroptosis in MDA-MB-231 cells. MDA-MB-231 cells were plated and treated with 5 μM pitavastatin with or without 50 μM DFO, which was added 2 h before pitavastatin treatment. (a, b) Total cell proteins were extracted to detect the expression of GPx4 and FSP1 through Western blotting with the internal reference GAPDH. (c) Morphological images were taken at 48 h and observed under TEM (30000 ×). The red arrow indicates autolysosomes. (d) Total cell proteins were extracted to detect the expression of LC3B and GAPDH was used as an internal reference. Error bars represented the mean ± SD of at least three independent experiments. *$P < 0.05$. (For interpretation of the references to colour in this figure legend, the reader is referred to the Web version of this article.)

gavage dose of 20 g mice as 0.1644, 0.00822, and 0.0822 mg [32]. Firstly, we subcutaneously injected MDA-MB-231 cells into female BALB/c nude mice breast pads and constructed tumor-bearing mice *in situ*. When the tumor volume was about 70 mm^3, the mice were randomly divided into four groups subjected to different protocols: Saline, Fluvastatin, Pitavastatin, and Simvastatin. Then daily gavage according to the calculated dose was administered and lasted for 20 days. We measured the body weight and tumor volume every two days. As shown in Fig. 7(a), the body weight of the mice in control group, Fluvastatin, Pitavastatin and Simvastatin-exposure group tended to increase stably in the 21 days during the experiment. As shown in Fig. 7(b), Fluvastatin, Pitavastatin, and Simvastatin reduced tumor volume by 30%, 58%, and 23% compared to the negative control, respectively. The mice were sacrificed on the 21st day and the tumors were taken out and photographed (Fig. 7(c)). The results showed that all three statins significantly reduced tumor volume and weight (Fig. 7(d) and (e)). We also conducted further research *in vivo* to confirm the key findings of the *in vitro* experiments. As shown in immunohistochemistry (IHC), statins reduced the percentage of Ki-67 positive cells in tumors, which is consistent with the inhibition of tumor growth (Fig. 7(f)). When exploring how statins induced ferroptosis in solid tumors, we specifically found that statins caused the accumulation of FSP1 and GPx4 in tumor cell membranes. This suggests that statins activate ferroptosis, upon which FSP1 and GPx4 are then recruited to the cell membrane to reduce membrane lipid peroxidation. Out of our expectation, statins led to an increase of HMGCR expression *in vivo* (Fig. 7(f)). These findings demonstrate that statin treatment led to a compensatory increment in HMGCR in tumor tissues, which may led by the degradation of HMGCR ubiquitination regulated by sterol was blocked [33]. Despite the increase in HMGCR expression, mevalonate pathway intermediates IPP, squalene, cholesterol and CoQ_{10} were all inhibited by pitavastatin in tumor tissues (Fig. 7(g)). These data demonstrated that the mevalonate pathway is critical for the initiation of ferroptosis induced by statins in TNBC cells. To evaluate the side effects of the doses of statins we used in this study, we performed H&E staining on the main organs of all mice. As shown in Fig. 8, the organs of the mice given the three statins did not show obvious abnormalities. The results of *in vivo* experiments revealed safe and effective anti-tumor properties of lipophilic statins, which have important guiding significance for clinical medication.

4. Discussion

As a newly raised form of cell death, ferroptosis has shown extensively significance in breast cancer [34]. The present study showed that pitavastatin is a potential ferroptosis-inducing agent. Through the TEM images of MDA-MB-231 cells treated with pitavastatin, we verified the morphological changes of mitochondria, indicating the occurrence of ferroptosis in these cells. Notably, many autolysosomes were observed in the TEM images, we then inferred that pitavastatin can induce excessive activation of autophagy in MDA-MB-231 cells. Autophagy is a highly conserved cellular process, which maintains cellular homeostasis via mediating the recycle of organelles and proteins. Furthermore, by regulating the mitochondrial number, autophagy can impactlipid metabolism, and thus influence ferroptosis [24]. The most widely accepted explanation for the relationship between autophagy and ferroptosis is that receptor co-activator 4 (NCOA4)-mediated ferritinophagy promotes ferroptosis by increasing the Fe^{2+} level [35,36]. Lipophagy, namely

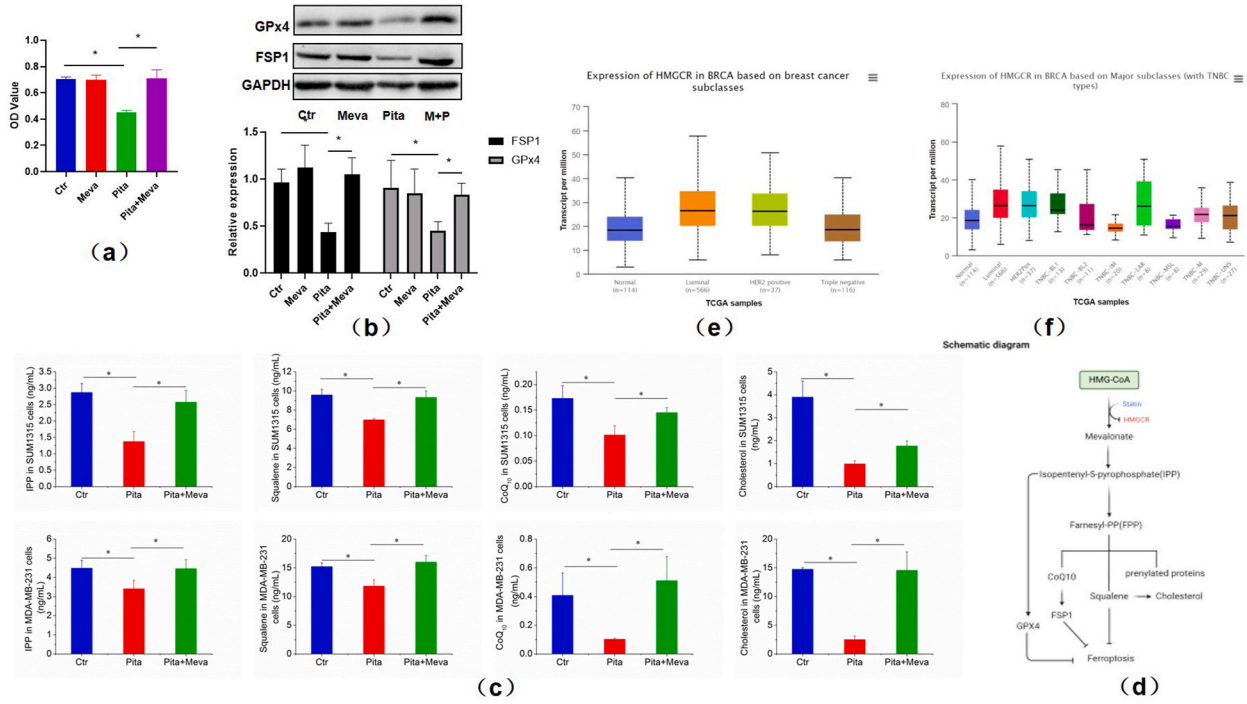

Fig. 6. Pitavastatin induces ferroptosis in MDA-MB-231 cells via the mevalonate pathway. MDA-MB-231 cells were plated and treated with 5 μM pitavastatin with or without 1 mM mevalonate, which was added 2 h before pitavastatin treatment.(a) Cell viability was assessed by CCK-8 assay at 48 h. (b) Western blotting was performed to detect the expression of GPx4 and FSP1 at 60 h, taking GAPDH as an internal reference. (c) Metabolomics analysis of mevalonate pathway intermediates isolated from extracts of either MDA-MB-231 cells or SUM1315 cells treated with 5 μM pitavastatin in the absence or presence of 1 mM mevalonate. (d) Schematic of the mevalonate pathway. (e) UALCAN was used to construct an expression profile of HMGCR in different subclasses of breast cancer. UALCAN analysis utilized TCGA-Assembler based on the TCGA level 3 RNA-seq database to download transcript per million (TPM) of breast cancer patients as a measure of expression [31]. (f) Detailed classification of TNBC showed that MSL TNBC patients emerged with much lower expression than others. Error bars represented the mean ± SD of at least three independent experiments. $^*P < 0.05$.

degradation of lipids via autophagy, promotes the production of free fatty acid, providing substrates for the subsequent lipid peroxidation during ferroptosis [37]. In addition, studies have shown that in "clockophagy", ARNTL degradation promotes ferroptosis by regulating HIF1α and activating lipid peroxidation [38]. Chaperone-mediated autophagy was reported to be able to lead to GPx4 degradation [39]. Based on these studies, we inferred that pitavastatin-mediated autophagy produced a large amount of Fe^{2+} and provide free fatty acids for lipid peroxidation, which finally induces ferroptosis. As for the interaction and mechanism between autophagy and ferroptosis activated by pitavastatin, further research is needed.

To reveal the molecular mechanisms, we first detected intracellular ROS levels and the GPx4 protein expression level. Our results indicated that GPx4 protein levels decreased, but the increase in ROS level was not rapid, hinting that pitavastatin did not directly inhibit GPx4 activity. Pitavastatin mainly induced ferroptosis through the regulation of GPx4 protein abundance. Ubiquinone, also called coenzyme Q_{10}, is representative of lipophilic metabolites known to transport electrons in mitochondrial respiratory chains. As one of the final metabolites of the MVA pathway, CoQ_{10} is a necessary substrate of FSP1 which has been discussed hereinbefore as a glutathione-independent ferroptosis suppressor. In the physiological system, CoQ_{10} can promote ferroptosis, making FSP1 essential because it can catalyze the reduction of ubiquinone coenzyme Q_{10} and subsequently protect cells from ferroptosis. Statins target the mevalonate pathway and inhibit the activity of CoQ_{10}. Our data showed that the protein level of FSP1 in MDA-MB-231 cells was decreased by pitavastatin, indicating that pitavastatin might induce ferroptosis through the non-mitochondrial FSP1 pathway in TNBC [40].

Within the previous ten years, studies have gradually established the anti-tumor efficiency of statins. Clinical data show that statin can improve local control and survival, reduce recurrence rate and mortality in patients with breast cancer [41,42]. Statins have been suggested to have a role in more aggressive breast cancer such as TNBC. Among women with nonmetastatic TNBC, initiation of statin therapy in the 12 months after breast cancer diagnosis was found to be statistically associated with improved overall survival (OS) and breast cancer-specific survival (BCSS) [43]. To achieve the application of statins in TNBC treatment, we should on one hand find greater understanding of ferroptosis to provide key insights into targeting ferroptosis in TNBC. And on the other hand, we need to develop biomarkers that accurately predict tumor response to ferroptosis induction. Statins can regulate breast cancer progression through the inhibition of proliferation, arrest of the cell cycle, and induction of apoptosis [19,20]. In particular, statins have specific effects on breast cancer cells, such as being even more effective on drug-resistant cells and TNBC cells. In colonic adenocarcinoma, liver

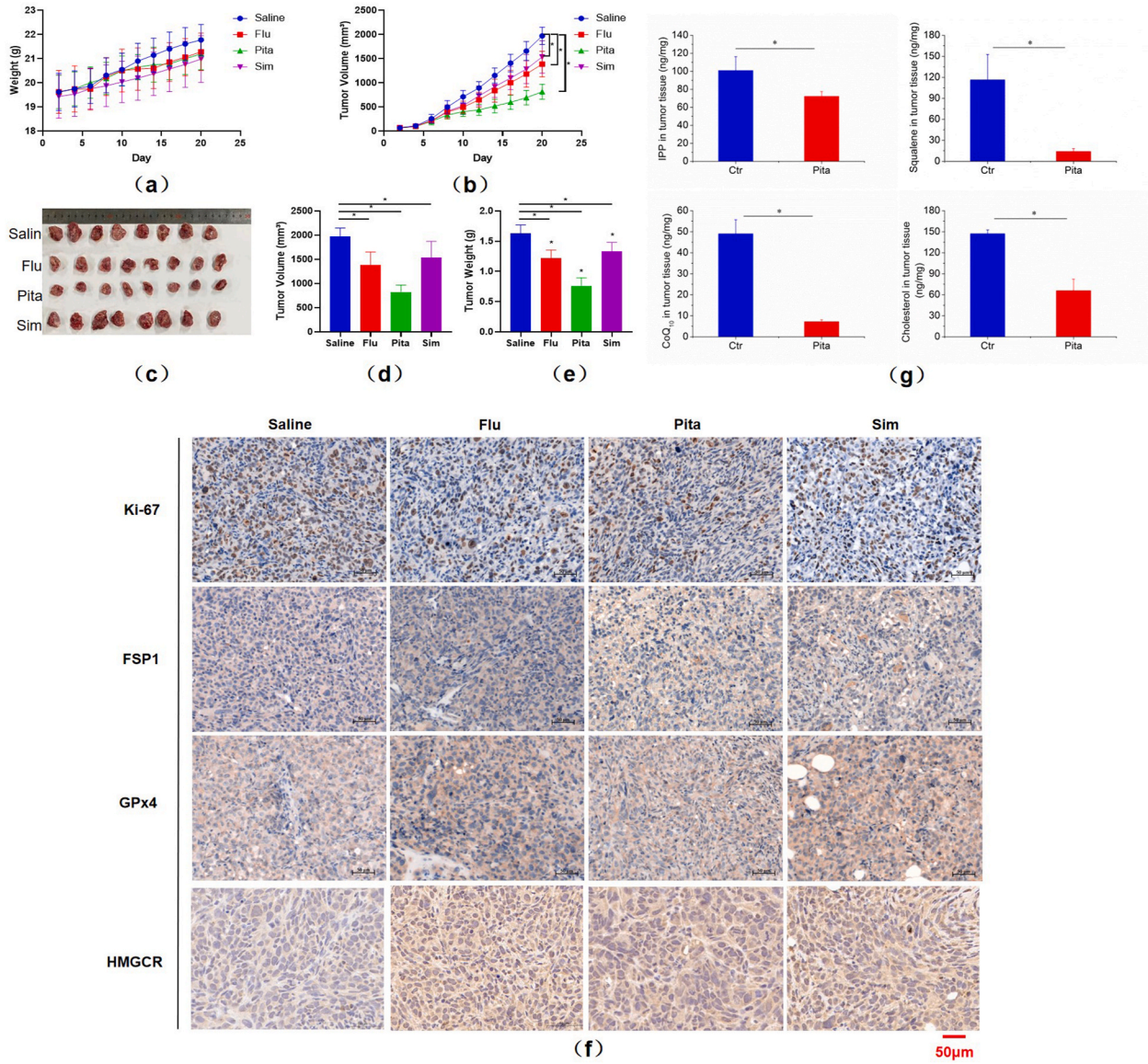

Fig. 7. Anti-tumor efficacy of statins *in vivo*. After oral administration, the body weight (a) and tumor volume (b) of four groups including Saline, Fluvastatin, Pitavastatin, and Simvastatin were recorded every three days (n = 8). (c) Image of the removed tumors. Statistical analyses of their effects on tumor volume (d) and weight (e) were conducted through GraphPad Prism 8.0; Error bars represented the mean ± SD of at least three independent experiments. *$P < 0.05$. (f) IHC of Ki-67, GPx4, and FSP1 on tumor tissues. The images are representative of each group under an optical microscope (200 ×). The scale bar represented 50 μm.

cancer and TNBC, p53 mutation up-regulates the expression of the mevalonate pathway related genes, indicating that mutational status of p53 is potential predictive biomarkers for statin treatment [44,45]. Simvastatin has been found to be a promising candidate to treat TNBC mediated by the PI3K/AKT pathway [46]. Another study found that through the MAPK pathway, statins can reduce the transcription factor ets proto-oncogene 1 (ets-1) expression via overexpression of dual specific protein phosphatase 4 (dusp4) [47]. Also, atorvastatin is reported to induce caspase-dependent apoptosis of TNBC cells via inhibiting matrix metalloproteinase (MMP)-2 and MMP-9 gene expression [48]. In our research, we found that statins have varying degrees of anti-cancer efficiency among different TNBC cells. By analyzing the data from different breast cancer subtypes in the TCGA database, we speculate that the mechanism of TNBC inhibition may be related to the expression level of HMGCR. Although this might hold some merits, TNBC inhibition is still likely related to other properties of the cell states. For example, studies have shown that the sensitivity of statins is related to the activation state of Akt. The activation of the Akt pathway caused by PTEN loss might be a potential mechanism for statin resistance [46]. In fact, ferroptosis induced by pitavastatin does not play a dominant role in all different TNBC cell lines. Studies have revealed that the high mesenchymal state exhibits dependence on the lipid peroxidase pathway [10,11]. This could explain why only MDA-MB-231 cells,

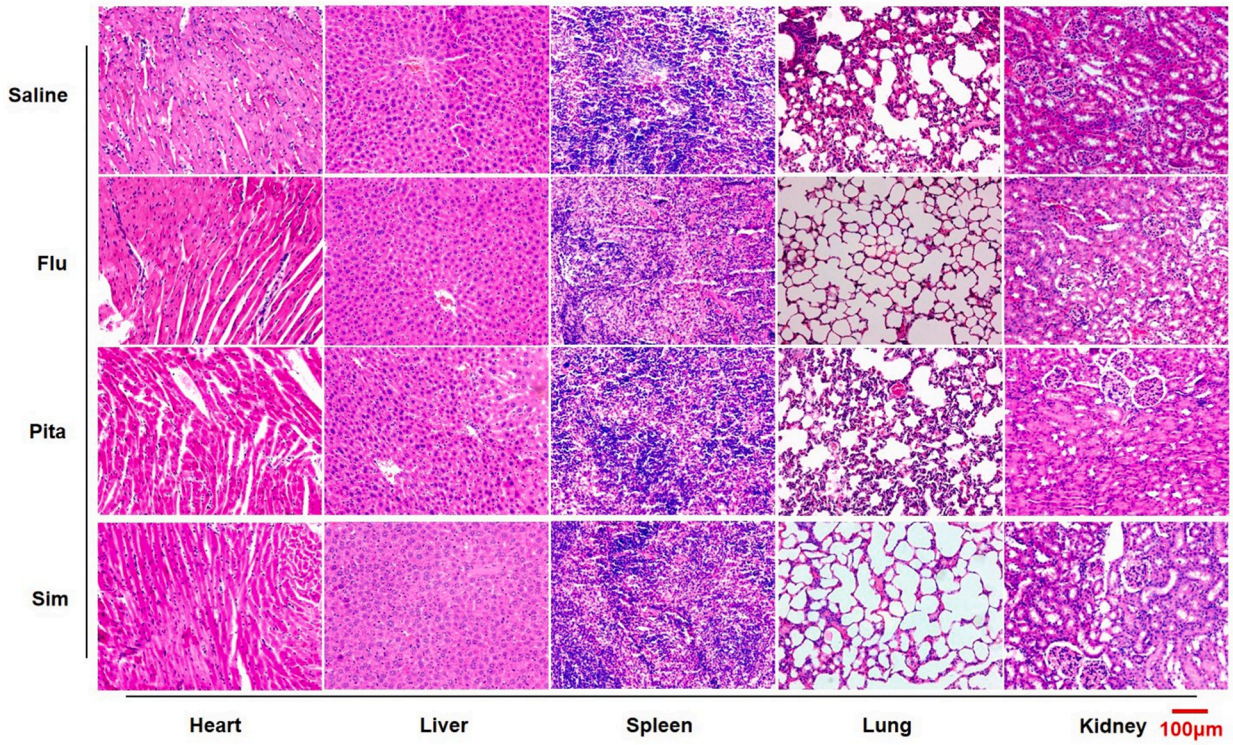

Fig. 8. H&E staining of heart, liver, spleen, lung, and kidney tissues of each group. H&E staining on the main organs of all mice was performed through paraffin sections. The images are representative of each group under an optical microscope (200 ×). The scale bar represented 100 μm. No organ damage or tumor metastasis was observed.

which are closely related to epithelial-mesenchymal transition (EMT) and the stemness phenotype, can temporarily induce ferroptosis by pitavastatin rather than other cell lines. Methods of identifying breast cancer patients who will benefit from statins need more clinical follow-up and statistics.

Ferroptosis has been recently found to act as a promising therapeutic target to manage cancer. There are very few the Food and Drug Administration (FDA)-approved drugs that can induce ferroptosis in tumor cells, let alone in clinical use. Statins are approved by FDA for the treatment of hypercholesterolemia and are effective at improving clinical outcomes when used for cardiovascular disease. We further investigated the anti-tumor effects of statins *in vivo* using safe oral doses recommended by FDA. We chose a TNBC tumor-bearing mouse model, and found that statins of safe doses could significantly inhibit tumor growth, without any obvious side effects in body weight and organs of mice. Subsequent tumor tissue analysis by IHC showed a decrease in Ki-67 positive cells, indicating lower TNBC cell proliferation in statins-treated groups. From the IHC images, we found the accumulation of FSP1 and GPX4 in tumor cell membranes, suggesting the occurrence of ferroptosis in solid tumors. Although in mouse studies, statins showed effective anti-cancer ability, the greater significance of ferroptosis inducers lies in the combination with existing therapeutics, including chemicals, targeted agents, radiotherapy, and also immunotherapy [49]. Our data hinted that a combination of statins and other anti-tumor drugs is a promising means of TNBC-treatment. In the future, we will use a patient-derived tumor xenograft (PDX) model for more accurate prediction of clinical outcomes of statins in treating TNBC patients. Moreover, integrating ferroptosis with emerging biotechnologies such as nanomaterials may amplify the anti-tumor effect and provide new opportunities.

In some cancer type, particularly in TNBC cells, ferroptosis is their vulnerability, which can be targeted to treat cancer. Our data show that TNBC cells to be more sensitive to statin-induced ferroptosis than their corresponding normal epithelial cells. These data suggest that there is an appropriate therapeutic window to selectively induce ferroptosis in TNBC without affecting normal tissues. Originally, the daily gavage doses of four statins in mice are objectively calculated by the daily oral therapeutic doses for human recommended by the FDA. We have searched for other publications and compared our administration and doses with them. The results indicate that a dose equivalent to cardiovascular protection can be effective [50,51]. Despite supported by the beneficial results of a large number of randomized controlled clinical trials, some studies have demonstrated that an overconsumption or prolonged use of statins may cause adverse reactions such as myopathy and hepatotoxicity [52]. The therapeutic regimen of the atorvastatin at a dose 80 mg/day therapeutic regimen has been found to cause |basal DNA damage in human lymphocytes [53,54]. Molecular mechanism studies suggested that oxidative stress is responsible for statin-induced possible adverse effects. These reports suggest that unpredictable side effects may be one of the greatest obstacles for the application of statins in cancer treatment. In our study, pitavastatin induces oxidative stress in MDA-MB-231 cells through the mitochondrial pathway, which may partially contribute to its anti-cancer

effect. Our data indicate that the IC50 value in HUVEC is much higher than TNBC cells and histomorphological study does not show obvious damage to the main organs of nude mice. The methodology of most *in vivo* statin safety studies is 8 week continuous treatment with once-daily administration of statins in the laboratory animals, while we only treated the mice for 3 weeks. Thus, more detailed study on statin safety is needed in order to provide important guidance for the clinical use of statins. Especially, studies can help to determine the therapeutic concentrations of statin that will not put TNBC patients with hyperlipidemia to a greater risk are urgently needed.

5. Conclusion

In summary, our study revealed that statins could inhibit cell proliferation, block the cell cycle, and induce cell death in TNBC cells *in vitro*. Particularly, the identification of ferroptosis induced by pitavastatin in MDA-MB-231 cells provided a new strategy for the treatment of refractory TNBC patients. We found that pitavastatin can induce ferroptosis in TNBC cells in an autophagy-dependent manner. *In vivo* experiments have further confirmed the clinical application prospects of statins in TNBC patients. We propose that this study can serve as a foundation for the research of ferroptosis-inducing agents and mechanisms involved in ferroptosis, whichoffers an opportunity for development of ferroptosis-based therapeutic strategies in TNBC.

Declaration of ethics

The animal study was reviewed and approved by Institutional Animal Care and Use Committee under No. IACUC-2008004 (Nanjing Medical University, Nanjing, China).

Consent for publication

Written informed consent for publication was obtained from all participants.

Data availability statement

Data are available on reasonable request. All data are available in the manuscript or supplementary documents.

Funding

The research was supported by the National Natural Science Foundation of China (No. 81872365, No. 81801827).

CRediT authorship contribution statement

Wen-Juan Tang: Writing – review & editing, Writing – original draft, Validation, Resources, Methodology, Investigation, Data curation, Conceptualization. **Di Xu:** Writing – review & editing, Software, Methodology, Investigation, Formal analysis, Data curation, Conceptualization. **Ming-Xing Liang:** Resources, Methodology, Investigation, Conceptualization. **Guan-Qun Wo:** Software, Resources, Methodology. **Wen-Quan Chen:** Methodology. **Jin-Hai Tang:** Project administration, Investigation, Funding acquisition, Conceptualization. **Wei Zhang:** Resources, Project administration, Methodology, Investigation, Funding acquisition, Conceptualization.

Declaration of competing interest

The authors declare that they have no known competing financial interests or personal relationships that could have appeared to influence the work reported in this paper.

Acknowledgments

We thank the Analysis and Testing Center of Nanjing Medical University for helping us make ultrathin sections. We thank the Pathology Group of the Jiangsu Provincial Hospital Core Facility Center for helping us make tissue sections.

Appendix A. Supplementary data

Supplementary data to this article can be found online at https://doi.org/10.1016/j.heliyon.2024.e27084.

References

[1] P. Kumar, R. Aggarwal, An overview of triple-negative breast cancer, Arch. Gynecol. Obstet. 293 (2) (2016) 247–269.
[2] R. Dent, M. Trudeau, K.I. Pritchard, W.M. Hanna, H.K. Kahn, C.A. Sawka, L.A. Lickley, E. Rawlinson, P. Sun, S.A. Narod, Triple-negative breast cancer: clinical features and patterns of recurrence, Clin. Cancer Res. 13 (15 Pt 1) (2007) 4429–4434.
[3] H. Kennecke, R. Yerushalmi, R. Woods, M.C. Cheang, D. Voduc, C.H. Speers, T.O. Nielsen, K. Gelmon, Metastatic behavior of breast cancer subtypes, J. Clin. Oncol. 28 (20) (2010) 3271–3277.
[4] M. Nedeljkovic, A. Damjanovic, Mechanisms of chemotherapy resistance in triple-negative breast cancer-how we can rise to the challenge, Cells 8 (9) (2019).
[5] C. Wang, S. Kar, X. Lai, W. Cai, F. Arfuso, G. Sethi, P.E. Lobie, B.C. Goh, L.H.K. Lim, M. Hartman, et al., Triple negative breast cancer in Asia: an insider's view, Cancer Treat Rev. 62 (2018) 29–38.
[6] S.J. Dixon, K.M. Lemberg, M.R. Lamprecht, R. Skouta, E.M. Zaitsev, C.E. Gleason, D.N. Patel, A.J. Bauer, A.M. Cantley, W.S. Yang, et al., Ferroptosis: an iron-dependent form of nonapoptotic cell death, Cell 149 (5) (2012) 1060–1072.
[7] J.R. Wu, Q.Z. Tuo, P. Lei, Ferroptosis, a recent defined form of critical cell death in neurological disorders, J. Mol. Neurosci. 66 (2) (2018) 197–206.
[8] K. Bersuker, J.M. Hendricks, Z. Li, L. Magtanong, B. Ford, P.H. Tang, M.A. Roberts, B. Tong, T.J. Maimone, R. Zoncu, et al., The CoQ oxidoreductase FSP1 acts parallel to GPX4 to inhibit ferroptosis, Nature 575 (7784) (2019) 688–692.
[9] S. Doll, F.P. Freitas, R. Shah, M. Aldrovandi, M.C. da Silva, I. Ingold, A. Goya Grocin, T.N. Xavier da Silva, E. Panzilius, C.H. Scheel, et al., FSP1 is a glutathione-independent ferroptosis suppressor, Nature 575 (7784) (2019) 693–698.
[10] M.J. Hangauer, V.S. Viswanathan, M.J. Ryan, D. Bole, J.K. Eaton, A. Matov, J. Galeas, H.D. Dhruv, M.E. Berens, S.L. Schreiber, et al., Drug-tolerant persister cancer cells are vulnerable to GPX4 inhibition, Nature 551 (7679) (2017) 247–250.
[11] V.S. Viswanathan, M.J. Ryan, H.D. Dhruv, S. Gill, O.M. Eichhoff, B. Seashore-Ludlow, S.D. Kaffenberger, J.K. Eaton, K. Shimada, A.J. Aguirre, et al., Dependency of a therapy-resistant state of cancer cells on a lipid peroxidase pathway, Nature 547 (7664) (2017) 453–457.
[12] S. Doll, B. Proneth, Y.Y. Tyurina, E. Panzilius, S. Kobayashi, I. Ingold, M. Irmler, J. Beckers, M. Aichler, A. Walch, et al., ACSL4 dictates ferroptosis sensitivity by shaping cellular lipid composition, Nat. Chem. Biol. 13 (1) (2017) 91–98.
[13] N.G. Vallianou, A. Kostantinou, M. Kougias, C. Kazazis, Statins and cancer, Anti Cancer Agents Med. Chem. 14 (5) (2014) 706–712.
[14] M. Osmak, Statins and cancer: current and future prospects, Cancer Lett. 324 (1) (2012) 1–12.
[15] L. Lacerda, J.P. Reddy, D. Liu, R. Larson, L. Li, H. Masuda, T. Brewer, B.G. Debeb, W. Xu, G.N. Hortobagyi, et al., Simvastatin radiosensitizes differentiated and stem-like breast cancer cell lines and is associated with improved local control in inflammatory breast cancer patients treated with postmastectomy radiation, Stem Cells Transl Med 3 (7) (2014) 849–856.
[16] Y. Shen, Y. Du, Y. Zhang, Y. Pan, Synergistic effects of combined treatment with simvastatin and exemestane on MCF-7 human breast cancer cells, Mol. Med. Rep. 12 (1) (2015) 456–462.
[17] B. Buranrat, W. Suwannaloet, J. Naowaboot, Simvastatin potentiates doxorubicin activity against MCF-7 breast cancer cells, Oncol. Lett. 14 (5) (2017) 6243–6250.
[18] S. Manthravadi, A. Shrestha, S. Madhusudhana, Impact of statin use on cancer recurrence and mortality in breast cancer: a systematic review and meta-analysis, Int. J. Cancer 139 (6) (2016) 1281–1288.
[19] A. Gopalan, W. Yu, B.G. Sanders, K. Kline, Simvastatin inhibition of mevalonate pathway induces apoptosis in human breast cancer cells via activation of JNK/CHOP/DR5 signaling pathway, Cancer Lett. 329 (1) (2013) 9–16.
[20] Y.Y. Shen, Y. Yuan, Y.Y. Du, Y.Y. Pan, Molecular mechanism underlying the anticancer effect of simvastatin on MDA-MB-231 human breast cancer cells, Mol. Med. Rep. 12 (1) (2015) 623–630.
[21] C.J. Sherr, Cancer cell cycles, Science 274 (5293) (1996) 1672–1677.
[22] K. Sinha, J. Das, P.B. Pal, P.C. Sil, Oxidative stress: the mitochondria-dependent and mitochondria-independent pathways of apoptosis, Arch. Toxicol. 87 (7) (2013) 1157–1180.
[23] D.J. Klionsky, Z.M.E. Al, Guidelines for the use and interpretation of assays for monitoring autophagy (3rd edition), Autophagy 1 (12) (2016).
[24] X. Chen, R. Kang, G. Kroemer, D. Tang, Broadening horizons: the role of ferroptosis in cancer, Nat. Rev. Clin. Oncol. 18 (5) (2021) 280–296.
[25] J.L. Goldstein, M.S. Brown, Regulation of the mevalonate pathway, Nature 343 (6257) (1990) 425–430.
[26] H. Mo, C.E. Elson, Studies of the isoprenoid-mediated inhibition of mevalonate synthesis applied to cancer chemotherapy and chemoprevention, Exp. Biol. Med. 229 (7) (2004) 567–585.
[27] J. Garcia-Bermudez, L. Baudrier, E.C. Bayraktar, Y. Shen, K. La, R. Guarecuco, B. Yucel, D. Fiore, B. Tavora, E. Freinkman, et al., Squalene accumulation in cholesterol auxotrophic lymphomas prevents oxidative cell death, Nature 567 (7746) (2019) 118–122.
[28] S. Borgquist, S. Djerbi, F. Ponten, L. Anagnostaki, M. Goldman, A. Gaber, J. Manjer, G. Landberg, K. Jirstrom, HMG-CoA reductase expression in breast cancer is associated with a less aggressive phenotype and influenced by anthropometric factors, Int. J. Cancer 123 (5) (2008) 1146–1153.
[29] S. Borgquist, A. Jogi, F. Ponten, L. Ryden, D.J. Brennan, K. Jirstrom, Prognostic impact of tumour-specific HMG-CoA reductase expression in primary breast cancer, Breast Cancer Res. 10 (5) (2008) R79.
[30] B.D. Lehmann, J.A. Bauer, X. Chen, M.E. Sanders, A.B. Chakravarthy, Y. Shyr, J.A. Pietenpol, Identification of human triple-negative breast cancer subtypes and preclinical models for selection of targeted therapies, J. Clin. Invest. 121 (7) (2011) 2750–2767.
[31] D.S. Chandrashekar, B. Bashel, S.A.H. Balasubramanya, C.J. Creighton, I. Ponce-Rodriguez, B. Chakravarthi, S. Varambally, UALCAN: a portal for facilitating tumor subgroup gene expression and survival analyses, Neoplasia 19 (8) (2017) 649–658.
[32] S. Reagan-Shaw, M. Nihal, N. Ahmad, Dose translation from animal to human studies revisited, Faseb. J. 22 (3) (2008) 659–661.
[33] S.Y. Jiang, H. Li, J.J. Tang, J. Wang, J. Luo, B. Liu, J.K. Wang, X.J. Shi, H.W. Cui, J. Tang, et al., Discovery of a potent HMG-CoA reductase degrader that eliminates statin-induced reductase accumulation and lowers cholesterol, Nat. Commun. 9 (1) (2018) 5138.
[34] Z. Li, L. Chen, C. Chen, Y. Zhou, D. Hu, J. Yang, Y. Chen, W. Zhuo, M. Mao, X. Zhang, et al., Targeting ferroptosis in breast cancer, Biomark. Res. 8 (1) (2020) 58.
[35] M. Gao, P. Monian, Q. Pan, W. Zhang, J. Xiang, X. Jiang, Ferroptosis is an autophagic cell death process, Cell Res. 26 (9) (2016) 1021–1032.
[36] W. Hou, Y. Xie, X. Song, X. Sun, M.T. Lotze, H.J. Zeh 3rd, R. Kang, D. Tang, Autophagy promotes ferroptosis by degradation of ferritin, Autophagy 12 (8) (2016) 1425–1428.
[37] Y. Bai, L. Meng, L. Han, Y. Jia, Y. Zhao, H. Gao, R. Kang, X. Wang, D. Tang, E. Dai, Lipid storage and lipophagy regulates ferroptosis, Biochem. Biophys. Res. Commun. 508 (4) (2019) 997–1003.
[38] M. Yang, P. Chen, J. Liu, S. Zhu, G. Kroemer, D.J. Klionsky, M.T. Lotze, H.J. Zeh, R. Kang, D. Tang, Clockophagy is a novel selective autophagy process favoring ferroptosis, Sci. Adv. 5 (7) (2019) eaaw2238.
[39] Z. Wu, Y. Geng, X. Lu, Y. Shi, G. Wu, M. Zhang, B. Shan, H. Pan, J. Yuan, Chaperone-mediated autophagy is involved in the execution of ferroptosis, Proc. Natl. Acad. Sci. U. S. A. 116 (8) (2019) 2996–3005.
[40] K. Shimada, R. Skouta, A. Kaplan, W.S. Yang, M. Hayano, S.J. Dixon, L.M. Brown, C.A. Valenzuela, A.J. Wolpaw, B.R. Stockwell, Global survey of cell death mechanisms reveals metabolic regulation of ferroptosis, Nat. Chem. Biol. 12 (7) (2016) 497–503.
[41] R.D. Van Wyhe, O.M. Rahal, W.A. Woodward, Effect of statins on breast cancer recurrence and mortality: a review, Breast Cancer 9 (2017) 559–565.
[42] Y.R. Li, V. Ro, L. Steel, E. Carrigan, J. Nguyen, A. Williams, A. So, J. Tchou, Impact of long-term lipid-lowering therapy on clinical outcomes in breast cancer, Breast Cancer Res. Treat. 176 (3) (2019) 669–677.
[43] M.K. Nowakowska, X. Lei, M.T. Thompson, S.F. Shaitelman, M.R. Wehner, W.A. Woodward, S.H. Giordano, K.T. Nead, Association of statin use with clinical outcomes in patients with triple-negative breast cancer, Cancer 127 (22) (2021) 4142–4150.
[44] S.H. Moon, C.H. Huang, S.L. Houlihan, K. Regunath, W.A. Freed-Pastor, JPt Morris, D.F. Tschaharganeh, E.R. Kastenhuber, A.M. Barsotti, R. Culp-Hill, et al., p53 represses the mevalonate pathway to mediate tumor suppression, Cell 176 (3) (2019) 564–580.e519.
[45] S. O'Grady, J. Crown, M.J. Duffy, Statins inhibit proliferation and induce apoptosis in triple-negative breast cancer cells, Med. Oncol. 39 (10) (2022) 142.

[46] Y.H. Park, H.H. Jung, J.S. Ahn, Y.H. Im, Statin induces inhibition of triple negative breast cancer (TNBC) cells via PI3K pathway, Biochem. Biophys. Res. Commun. 439 (2) (2013) 275–279.
[47] H.H. Jung, S.H. Lee, J.Y. Kim, J.S. Ahn, Y.H. Park, Y.H. Im, Statins affect ETS1-overexpressing triple-negative breast cancer cells by restoring DUSP4 deficiency, Sci. Rep. 6 (2016) 33035.
[48] F. Bakar-Ates, E. Ozkan, Atorvastatin induces downregulation of matrix metalloproteinase-2/9 in MDA-MB-231 triple negative breast cancer cells, Med. Oncol. 40 (1) (2022) 22.
[49] Y. Wu, C. Yu, M. Luo, C. Cen, J. Qiu, S. Zhang, K. Hu, Ferroptosis in cancer treatment: another way to rome, Front. Oncol. 10 (2020) 571127.
[50] Y. Kojima, T. Ishida, L. Sun, T. Yasuda, R. Toh, Y. Rikitake, A. Fukuda, N. Kume, H. Koshiyama, A. Taniguchi, et al., Pitavastatin decreases the expression of endothelial lipase both in vitro and in vivo, Cardiovasc. Res. 87 (2) (2010) 385–393.
[51] S. Malik, A.K. Sharma, S. Bharti, S. Nepal, J. Bhatia, T.C. Nag, R. Narang, D.S. Arya, In vivo cardioprotection by pitavastatin from ischemic-reperfusion injury through suppression of IKK/NF-κB and upregulation of pAkt-e-NOS, J. Cardiovasc. Pharmacol. 58 (2) (2011) 199–206.
[52] A. Liu, Q. Wu, J. Guo, I. Ares, J.L. Rodriguez, M.R. Martinez-Larranaga, Z. Yuan, A. Anadon, X. Wang, M.A. Martinez, Statins: adverse reactions, oxidative stress and metabolic interactions, Pharmacol. Ther. 195 (2019) 54–84.
[53] G. Gajski, V. Garaj-Vrhovac, Application of cytogenetic endpoints and comet assay on human lymphocytes treated with atorvastatin in vitro, J Environ Sci Health A Tox Hazard Subst Environ Eng 43 (1) (2008) 78–85.
[54] G. Gajski, V. Garaj-Vrhovac, V. Orescanin, Cytogenetic status and oxidative DNA-damage induced by atorvastatin in human peripheral blood lymphocytes: standard and Fpg-modified comet assay, Toxicol. Appl. Pharmacol. 231 (1) (2008) 85–93.